UDC 551.509.313

THE EFFECT OF INITIAL UNCERTAINTIES ON PREDICTIONS MADE WITH SOME BAROTROPIC AND BAROCLINIC MODELS [1]

MADHAV L. KHANDEKAR [2]
Florida State University, Tallahassee, Fla.

ABSTRACT

A statistical theory developed previously is applied to predictions made with three simple atmospheric models under similar boundary and initial conditions. The theory gives minimum variances in height fields of various isobaric levels. The governing equations of each model are utilized to transform these initial variances to final variances of forecast fields. These variances are a measure of the theoretical minimum errors expected at any future states due to presence of initial uncertainties. Using the normal frequency function, these theoretical variances are further transformed to probabilities of obtaining forecast heights within specified magnitudes of true heights. These theoretical probabilities are compared with observed probabilities of errors in forecast fields obtained by various models for three synoptic situations.

The theoretical probabilities are found to be larger everywhere than the observed ones, in support of the statistical theory that provides limiting probabilities not to be exceeded. A comparison of theoretical minimum variances indicates that the growth of these variances is more pronounced in more complex models that incorporate additional terms in the governing equations. The effect of hypothetically increasing the number of reporting stations indicates that a substantial reduction in initial and final variances is realized when the number of reporting stations is increased by two to three times the present number.

The results of this study offer a possibility of choosing an optimum model to obtain the most reliable short-range weather prediction for a given synoptic situation.

1. INTRODUCTION

It has been long realized that lack of complete information concerning the intitial state of the atmosphere contributes to inaccuracies in the prediction of future states. A quantitative assessment of these inaccuracies would be very essential in connection with the problem of atmospheric predictability. In recent years, attempts have been made to estimate the effect of initial uncertainty on the predictability of atmospheric parameters by considering simple numerical models (for example, Thompson 1957, Lorenz 1963). A network sampling theory that provides theoretical minimum error distributions for predicted meteorological parameters has been developed by Gleeson (1961). In previous studies, this theory was applied to obtain minimum variances for predictions made with a simple barotropic model (Gleeson 1964) and with a spectral form of the barotropic vorticity equation (Stewart 1967).

The purpose of the present study is to make an intermodel comparison of theoretical minimum errors expected at any future states due to presence of initial uncertainties. For this comparison, a simple barotropic, a three-level quasi-geostrophic, and a two-level balance model are chosen. Using data from three synoptic situations, theoretical minimum variances of height fields at various isobaric levels are calculated by a procedure described in the next section. The growth of these variances with time and their dependence on various assumptions of the models are discussed in section 5. Finally, possible implications of these results for developing a criterion for optimum modeling of the atmosphere are also considered.

2. ANALYSIS ERRORS

The network sampling theory mentioned earlier enables us to obtain the variance of the error at any point in a two-dimensional analysis of a meteorological parameter. In this development, values interpolated from synoptic analysis are regarded as measurements. For example, consider a map on which synoptic values of a parameter q have been plotted. After the map has been analyzed, one can interpolate a value of q at any point. An interpolated value of q at any point (not necessarily a station location) in general differs from the true value by an amount Δq, which is the error in measuring q at that point. Now, imagine that the true pattern of q occurs an indefinitely large number of times; that the locations of observations are distributed independently and randomly relative to the pattern each time; and that different analysts make independent analyses of the q field everytime the pattern recurs. By means of a statistical argument (Gleeson 1961), it is possible to write the variance σ_q^2 of the interpolated value of q at a point as

$$\sigma_q^2=0.056a\left(\frac{\partial\hat{q}}{\partial x}\right)^2. \tag{1}$$

Here, $(\partial\hat{q}/\partial x)$ is the true gradient of q at the point, and a is the square of the average distance between reporting stations over the region of analysis.

We see from this equation that in a region of tight gradient, if we displace the isopleths in our analysis by even a relatively small amount, there will be a significant error in the interpolated value of q at that point. Further, it is

[1] Research supported by the Section on Atmospheric Sciences, National Science Foundation, NSF Grant GA-1007.

[2] Presently a National Research Council Fellow at the Meteorological Service of Canada, Toronto.

logical that the variance of q should be larger or smaller as the average distance between reporting stations is larger or smaller.

This theory gives minimum variance because it does not consider errors in observations, systematic errors, or errors in the physical model. From the equation pertaining to a forecast model, a corresponding variance equation can be obtained to calculate the variance of the variable q at any future time (see the appendix for further details).

3. MODELING EQUATIONS

In this study, we have used three simple models that can be described briefly by the following equations.

The simplest of the barotropic models for horizontal and nondivergent flow can be expressed by the simplified form of the vorticity equation

$$\frac{\partial \zeta}{\partial t}=-\mathbf{V}\cdot\nabla(\zeta+f). \tag{2}$$

Here, the symbols have standard meanings. The horizontal wind vector $\mathbf{V}$ is expressed using a quasi-geostrophic assumption as

$$\mathbf{V}=\frac{g}{\bar{f}}\mathbf{k}\times\nabla z$$

where $\bar{f}$ is the mean value of the Coriolis parameter over the region of analysis. Writing ζ in terms of z, the height of a constant pressure surface, we have

$$\nabla^2\left(\frac{\partial z}{\partial t}\right)=-J\left(z,\frac{g}{\bar{f}}\nabla^2 z+f\right). \tag{3}$$

Using a suitable finite-difference grid, one can solve this equation numerically, and integration can be carried out in suitable time steps to obtain z values at any future time at 500 mb, the assumed level of nondivergence.

The second model considered here is a three-level quasi-geostrophic model for which the vorticity equation can be written in the form

$$\nabla^2\left(\frac{\partial z}{\partial t}\right)=-J(z,\eta)+\frac{\bar{f}^2}{g}\frac{\partial \omega}{\partial p}. \tag{4}$$

Here, $\omega=dp/dt$ is the vertical velocity in the p-coordinate system. Making use of the thermodynamic equation consistent with the quasi-geostrophic assumption and eliminating the time-dependent term between that and the vorticity equation, we have the consistent omega equation for this model as

$$\sigma\nabla^2\omega+\bar{f}^2\frac{\partial^2\omega}{\partial p^2}=g\frac{\partial}{\partial p}[J(z,\eta)]-\frac{g^2}{\bar{f}}\nabla^2 J\left(z,\frac{\partial z}{\partial p}\right). \tag{5}$$

Here, $\sigma=-(\alpha/\theta)(\partial\theta/\partial p)$, the static stability, is kept constant on an isobaric surface and is allowed to vary only in the vertical. The omega equation is applied at the 400- and 600-mb levels, while the vorticity equation is applied at the 300-, 500-, and 700-mb levels, respectively (see fig. 1). For solution of the omega equation, the vertical

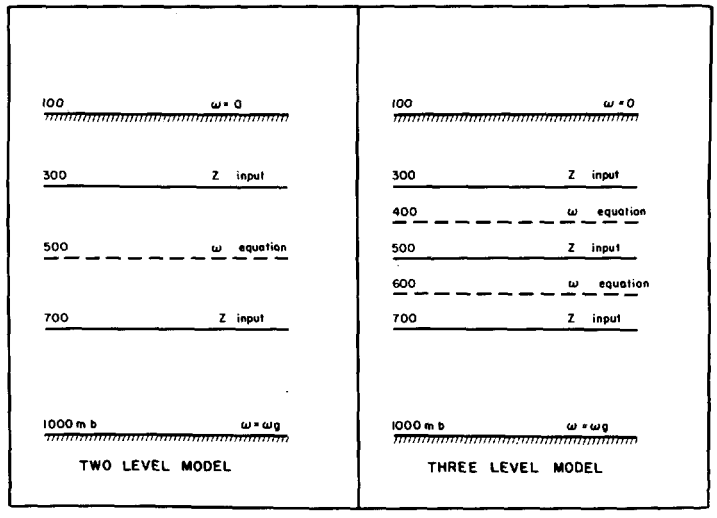

FIGURE 1.—Vertical grid for two- and three-level models.

boundary conditions are

$$\omega=0 \text{ at } p=100 \text{ mb}$$

and

$$\omega=\omega_g \text{ at } p=1000 \text{ mb}.$$

Following Cressman (1960), we obtain the values of ω_g at 1000 mb as a sum of terrain induced and frictionally induced vertical velocities. On the lateral boundary, ω is kept zero everywhere at all times.

The third model chosen here is a two-level balance model in which we make use of a balance equation obtained from the divergence equation as

$$\nabla\cdot(f\nabla\psi)+2J(u_\psi,v_\psi)=\nabla^2\phi \tag{6}$$

where ϕ is the geopotential, ψ the stream function, and u_ψ and v_ψ are the rotational parts of the wind components u, v, respectively. As a special form of this equation, the Jacobian term is neglected to give a linearized balance equation as

$$\nabla\cdot(f\nabla\psi)=\nabla^2\phi. \tag{7}$$

The consistent vorticity equation corresponding to this linearized balance filter can be written following Lorenz (1960) as

$$\nabla^2\left(\frac{\partial\psi}{\partial t}\right)=-\mathbf{V}\psi\cdot\nabla\eta+f\frac{\partial\omega}{\partial p}-\nabla\chi\cdot\nabla f. \tag{8}$$

Using a consistent thermodynamic equation, we obtain the corresponding omega equation as

$$\sigma\nabla^2\omega+f^2\frac{\partial^2\omega}{\partial p^2}=f\frac{\partial}{\partial p}[J(\psi,\eta)]-\nabla^2\left[J\left(\psi,\frac{\partial\phi}{\partial p}\right)\right]$$
$$+f\frac{\partial}{\partial p}[\nabla\chi\cdot\nabla f]-\frac{\partial^2}{\partial p\partial t}\nabla f\cdot\nabla\psi-\nabla^2\left[\nabla\chi\cdot\nabla\frac{\partial\phi}{\partial p}\right]. \tag{9}$$

This equation has five forcing functions as compared to two in the usual quasi-geostrophic omega equation (5). Besides the first two terms, namely, the differential vor-

ticity advection and the Laplacian of the thermal advection, the remaining three terms arise due to the divergent part of the wind and the variation of the Coriolis parameter. These terms cannot be explicitly evaluated; hence, the solution of this equation is obtained by an iterative procedure similar to the one used by Gates and Riegel (1963). After obtaining a convergent solution of ω, the vorticity equation (8) can be solved, and numerical integration can be carried out to obtain forecast heights at any future time.

For each of these models, the variance equation is developed by the procedure discussed earlier and is solved by numerical techniques to obtain variances of the height fields at any future time.

4. RESULTS AND DISCUSSIONS

The calculations are performed on a rectangular grid chosen on a polar stereographic projection, true at 60° N. The grid is extended to cover a major portion of the Northern Hemisphere to minimize the boundary condition errors and at the same time to examine the large-scale atmospheric flow. A grid distance of 500 km (about 4.5° of latitude) is chosen in the x and y directions. The average distance between observing stations over the regions covered by the grid is about 570 km; hence, a grid distance of 500 km is chosen as it enables us to calculate the theoretical variances under certain assumptions. There are 27 grid points in the x direction and 25 in the y direction with 36 grid points chopped off in each of the southeast and southwest corners of the North American Continent as these regions are over oceans where there are hardly any data points (fig. 2).

Three synoptic situations were chosen to obtain forecast and variance fields by each model. Since the objective is to compare errors encountered with barotropic as well as baroclinic models, the synoptic situations chosen were such as to show strong baroclinic development in subsequent 24 to 48 hr. As an example, we present briefly some of the verification results for the synoptic situation of Jan. 25, 1964, for which the initial input field at 500 mb is shown in figure 3. The 24-hr forecast fields (solid lines) obtained by the three models are presented in figures 4 to 6. In each case, the forecast field is superimposed on the verification field (dashed lines) for comparison. The barotropic model merely advects the field without any intensification and has placed the main trough located over the central United States about half way between its initial and verifying position. The forecast fields obtained by the two baroclinic models are shown in figures 5 and 6. Both these fields are more or less alike, showing some improvement in the predicted position of the main trough as compared with the barotropic model; however, none of the two baroclinic models predicted any significant development of the system as portrayed in the verification field.

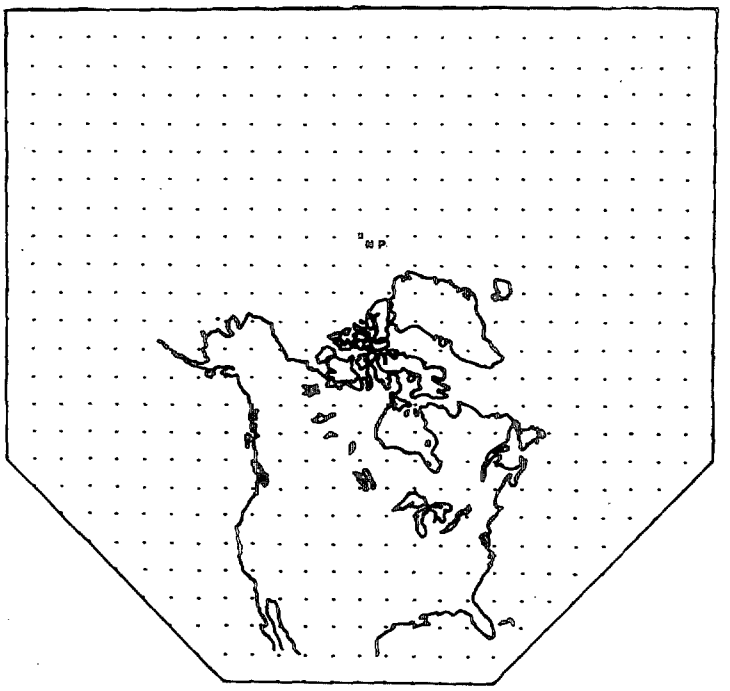

FIGURE 2.—Basic grid showing the outlines of North America and adjoining regions. Dots refer to grid points and NP denotes the North Pole.

The verification of forecast fields for the remaining two synoptic situations showed similar results. Both the baroclinic models showed some improvement over the barotropic model in the predicted position of the major systems, but none of them indicated any significant development of the systems.

COMPARISON OF OBSERVED AND THEORETICAL ERROR DISTRIBUTIONS

For each model, the variance equation is derived from the governing vorticity equation. For example, consider the simple barotropic equation (2) for which the variance equation is given by (13) as developed in the appendix. This variance equation is solved by the standard relaxation technique to yield the variance of the height tendency, that is, $\sigma^2(\partial z/\partial t)$, at any time step; this together with (16) enables us to obtain the minimum variances of the height field at any future time. Further, from the forecast height field, we obtain height errors at any future time for which the verification field is available. Constructing a frequency distribution of these errors, we obtain relative frequencies of height errors to be within specified magnitudes $|\Delta z|$. For a specified value of $|\Delta z|$, theoretical values of $\sigma^2(z_i)$ at any future time t can be converted to theoretical probability P, using tables of the normal distribution. These are averaged over the verification region to obtain

$$\overline{P}=\sum_{i=1}^{N} P_i/N$$

where $N=369$ grid points over the verification region and

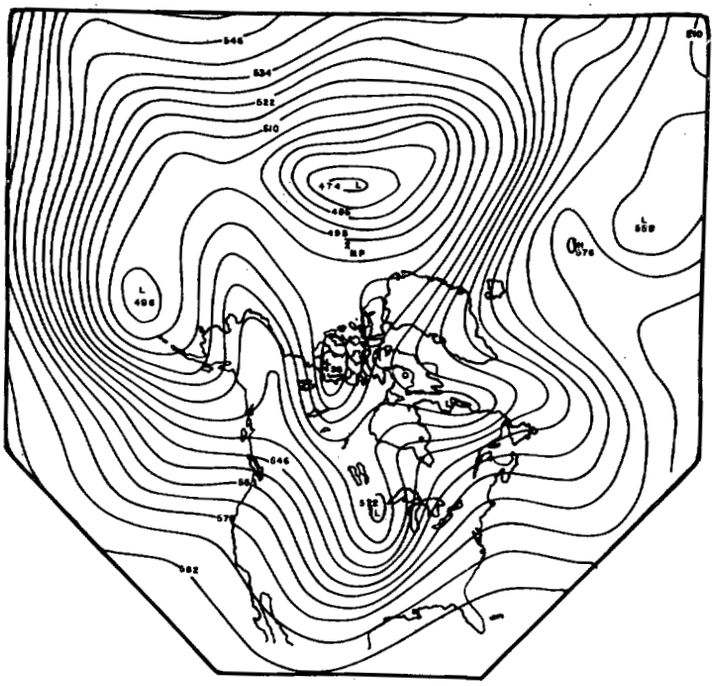

FIGURE 3.—Height field at 500 mb at 00 GMT on Jan. 25, 1964. The contour interval is 60 m.

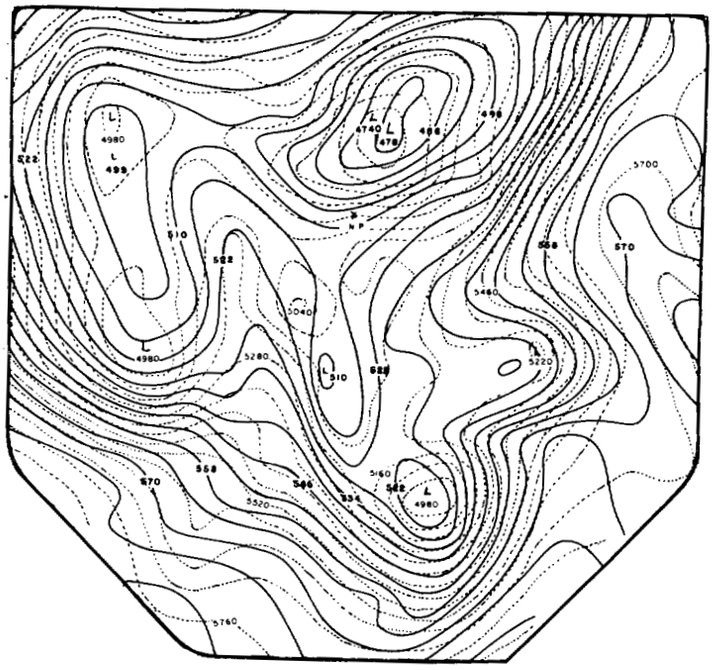

FIGURE 5.—Same as figure 4, but for the three-level quasi-geostrophic model.

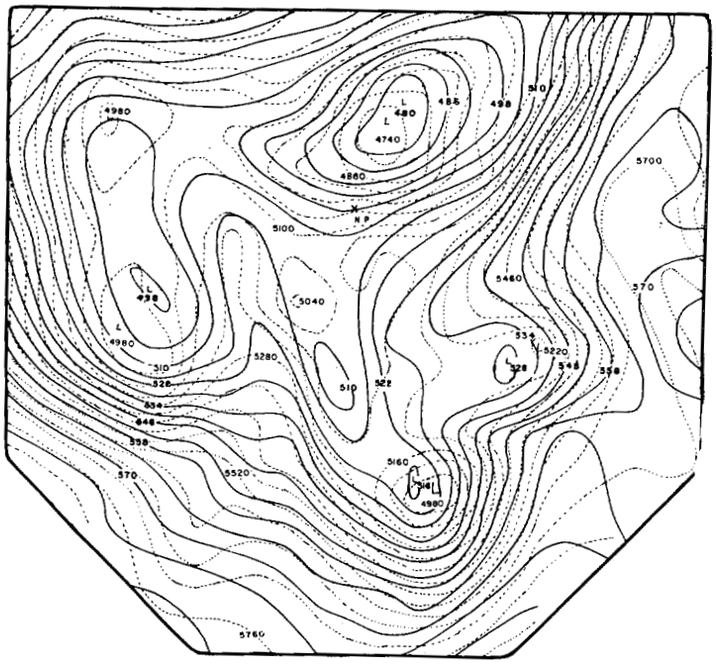

FIGURE 4.—Twenty-four-hour forecast field (solid lines) at 500 mb obtained by the simple barotropic model, superimposed on verification field at 00 GMT on Jan. 26, 1964 (dashed lines). Solid lines are labeled in tens of meters and dashed lines in full meters.

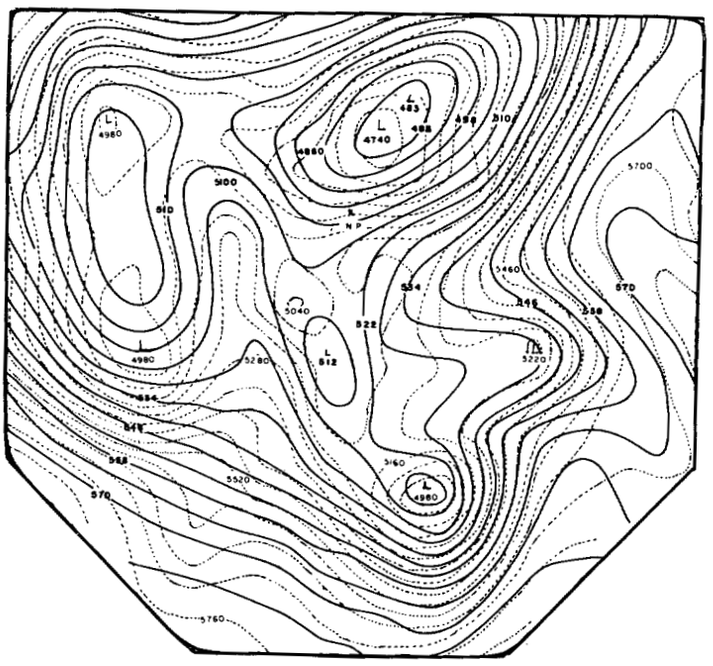

FIGURE 6.—Same as figure 4, but for the two-level balance model.

$\overline{P}$ is the "expected" or average limiting probability for forecast heights to be in error by no more than $|\Delta z|$. Using these values, one can construct a graph of limiting (theoretical) probabilities versus Δz (in meters). Similarly, cumulative (observed) frequencies of height errors in the forecast fields are also plotted. Figure 7 shows these sets of theoretical (solid lines) and observed (dashed lines) curves at various levels for the synoptic situation of Jan. 25, 1964. The verification is made for 24-hr forecasts obtained by the three-level quasi-geostrophic model. For comparison, the curves for persistence forecasts—if the initial information is presented as a forecast—are also

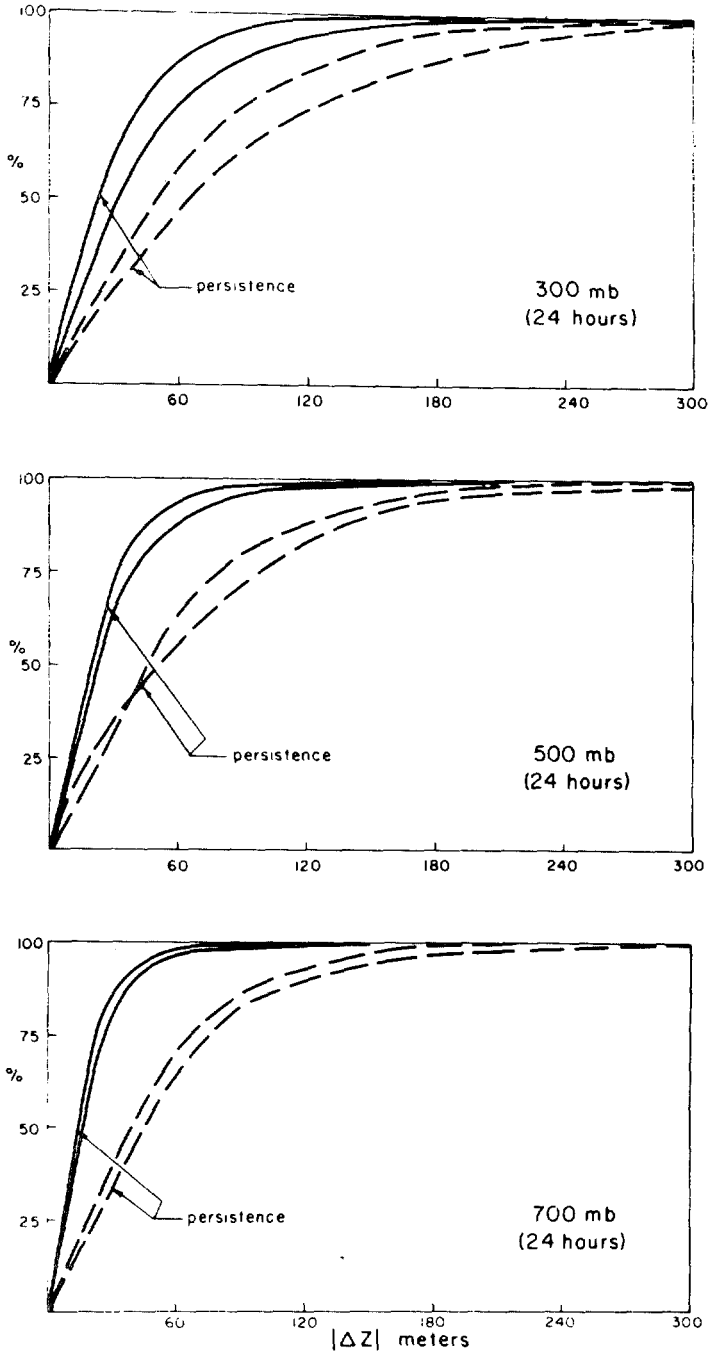

FIGURE 7.—Observed (dashed lines) and theoretical (solid lines) cumulative error distributions for 24-hr forecast heights obtained by the three-level quasi-geostrophic model. Initial data, 00 GMT on Jan. 25, 1964.

plotted and labeled accordingly. (The theoretical curve for persistence forecasts is obtained by transforming the initial variances to average limiting probabilities, while the corresponding observed curve is obtained by simply constructing a frequency distribution of height errors between the initial and the verifying fields.) We see first of all that the theoretical curve is everywhere above the observed curve, which is in support of our argument that the theoretical probabilities are not to be exceeded. Further, the theoretical curve at each level is lower than the corresponding persistence curve, since the integration in time adds to the initial variance. The observed curve is, in general, higher than the corresponding persistence curve, indicating the gain in accuracy of forecast by the model over persistence. The curves for 48-hr verification for the same synoptic situation are shown in figure 8 and indicate similar results. The theoretical curves here are much lower than the corresponding persistence curves, since integration over a longer period has added more to the initial variances. The observed curves at all levels approach the persistence curves, indicating the deterioration of forecasts with time. In this study, forecast and variance fields were obtained up to a period of 48 hr only. As integration is carried over longer periods, we expect the theoretical as well as the observed curves for a model to drop constantly and reach the level of persistence.

The comparison of observed and theoretical error distributions for the remaining two synoptic situations showed similar results, indicating that the theoretical probabilities were largest in all cases.

5. GROWTH OF THEORETICAL VARIANCES WITH TIME

An analysis of variance was made, using the average variance over the verification region to get a quantitative assessment of the growth of theortical variances with time.

Consider equation (16) in the appendix; the equation gives the variance at any grid point at the end of $2K$ hours as

$$\sigma^2(z_{2K})=\sigma^2(z_0)+4T^2\sum_{i=1}^{K}\sigma^2\left(\frac{\partial z}{\partial t}\right)_{2i-1}.$$

Here, $\sigma^2(z_0)$ is the initial variance of the z field, T is the constant time step, and $\sigma^2(\partial z/\partial t)_i$ is the variance of the height tendency at the ith time step. With $K=24$, we obtain the variance at the end of the 48-hr period as

$$\sigma^2(z_{48})=\sigma^2(z_0)+4T^2\sum_{i=1}^{24}\sigma^2\left(\frac{\partial z}{\partial t}\right)_{2i-1}.$$

This can be written as

$$\sigma^2(z_{48})=\sigma^2(z_0)+4T^2\sum_{i=1}^{12}\sigma^2\left(\frac{\partial z}{\partial t}\right)_{2i-1}+4T^2\sum_{i=13}^{24}\sigma^2\left(\frac{\partial z}{\partial t}\right)_{2i-1}. \quad (10)$$

Taking $\sigma^2(z_{48})$, the variance at the end of the 48-hr period, as the total variance, we see that this total variance is made up of three terms as expressed on the right-hand side of (10). These three terms are respectively the initial variance, the contribution through the time integration for the first 24-hr period, and the corresponding contribution for the subsequent 24-hr period. Equation (10) is averaged over the verification area (369 grid points), and the average variances (in meters^2) of the three terms on the right-hand side are obtained for all the three models at various levels. Table 1 shows these average variances for the three synoptic situations.

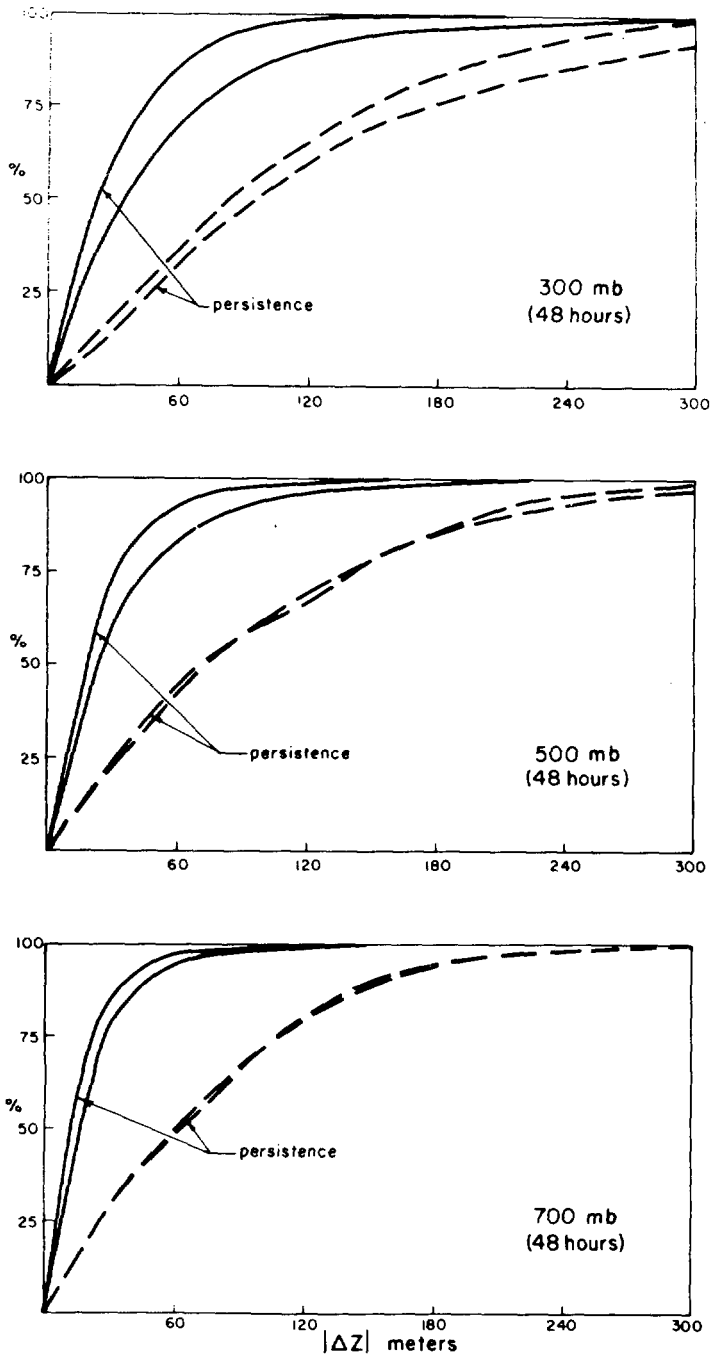

FIGURE 8.—Same as figure 7, but for 48-hr forecast heights verifying at 00 GMT on Jan. 27, 1964.

TABLE 1.—*Analysis of variance of 24- and 48-hr forecasts for various models**

Date and model	Level	$\overline{\sigma^2(z_0)}$	$\overline{4T^2 \sum_{i=1}^{12} \sigma^2 \left(\frac{\partial z}{\partial t}\right)_{2i-1}}$	$\overline{4T^2 \sum_{i=13}^{24} \sigma^2 \left(\frac{\partial z}{\partial t}\right)_{2i-1}}$
Jan. 25, 1964	(mb)	(m²)		
Barotropic	500	952	767	699
Three-level quasi-geostrophic	300	1692	2198	1789
	500	952	751	634
	700	437	139	115
Two-level balance	300	1692	2285	2223
	700	437	142	152
Dec. 7, 1963				
Barotropic	500	753	390	402
Three-level quasi-geostrophic	300	1388	1549	1627
	500	753	401	438
	700	309	60	72
Two-level balance	300	1388	1791	2770
	700	309	66	91
Jan. 6, 1962				
Barotropic	300	1007	907	1098
Three-level quasi-geostrophic	300	1856	2613	3186
	500	1007	914	1112
	700	538	240	262
Two-level balance	300	1856	2463	3300
	700	538	235	386

*The (theoretical) total variance $\sigma^2(z_{48})$ is partitioned into three components as shown in equation (10) and then averaged over the verification area. These average variances (meters²) of the three components are shown in columns 3, 4, and 5 for the three synoptic situations under study.

We see from this table that the initial variance explains a major portion of the total variance in lower levels, especially at 700 mb where the contribution from the time integration term is smaller because of the overall weaker gradients at that level. At 300 mb, the contribution from the time integration term is quite considerable as a result of tighter gradients at this level. Further, in the case of the two-level balance model, the contribution from the time integration term is generally more pronounced due to the inclusion of additional terms in the vorticity equation, namely, the divergence term and the $\nabla\chi \cdot \nabla f$ term. In general, the contribution to the total variance by various terms depends on the magnitude of the term itself and the way it is evaluated by finite-difference approximations. The advection term, being the largest term, contributes most to the growth of the variance. The divergence term is of a smaller order of magnitude; and further, its incorporation through vertical finite differencing appears to contribute the least. The additional term $\nabla\chi \cdot \nabla f$ has about the same order of magnitude as the divergence term but seems to contribute more than the divergence term, since it is evaluated using horizontal finite differences on an isobaric surface. This leads to additional growth of variance for the two-level balance model. Further, the growth rates of individual grid points lying in the vicinity of an intense trough are found to be much more pronounced as a result of strong gradients associated with the trough. A typical pattern of such a growth rate is presented in figure 9 where the values of final standard deviation for a selected grid point are plotted against time for various models. Here, the curves are obtained using the data of Jan. 25, 1964, and the grid point selected lies ahead of the main trough located over the central United States (fig. 3). We see that the standard deviation steadily increases at all levels, the growth being most pronounced at the 300-mb level. Consider the two curves at the 500-mb level. The lower curve is obtained from the simple barotropic model, in which the growth of standard deviation is due to the presence of the advection term only, while the upper curve is obtained from the three-level quasi-geostrophic model where the additional increase in variance is due to the inclusion of the divergence term at that level. Considering further the two sets of curves at 300 and 700 mb, we see that the additional increase in the standard deviation shown by the dashed curves is due to the presence of

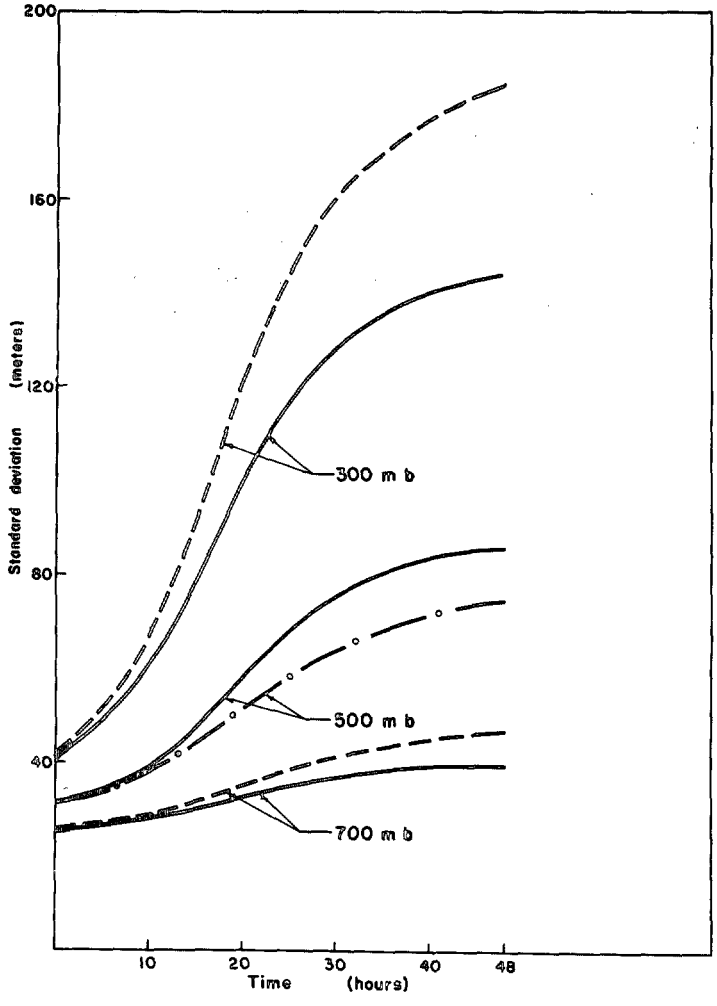

FIGURE 9.—Growth of standard deviation (in meters) of geopotential height error with time for a selected grid point. Dashed lines with dots, barotropic model; solid lines, three-level quasi-geostrophic models; dashed lines, two-level balance model; initial data, Jan. 25, 1964.

the $\nabla\chi \circ \nabla f$ term appearing in the two-level balance model. At 500 mb, the initial standard deviation of 32 m grows to 75 m with the simple barotropic model and further to 86 m with the three-level quasi-geostrophic model. At 300 mb, the initial standard deviation of 41 m grows to 141 m with the quasi-geostrophic model and further to 184 m with the balance model.

This variation of the standard deviation indicates how the initial uncertainty grows with time, making the forecast fields more unreliable as integration is carried over longer periods. Further, the growth of initial uncertainty is found to be more pronounced in more complex models, thus indicating that increasing complexities of a model, in general, tend to increase the growth of initial uncertainty and thus may counteract to some extent any possible improvement in accuracy that might be expected in return. This leads us to the problem of atmospheric predictability and the possibility of long-range deterministic prediction. Recent theoretical studies (Lorenz 1963) and numerical experiments (Leith 1964, Mintz 1965) have suggested that "the limit for deterministic predictability of the atmosphere is about 2 weeks in winter and somewhat longer in summer." Lorenz further suggested that in a real atmosphere this limit may be more likely 2 to 3 days. More recently, Gleeson (1967) has shown that errors in deterministic prediction of a meteorological variable do not remain small but eventually become large enough for the predicted variable to be completely uncertain within its range of possible values. The calculations made here, using data from three synoptic situations, seem to suggest that the limit for deterministic predictability is reached in relatively shorter time for more complex models. From table 1, we see that, for the two-level balance model, the average initial variance at 300 mb increases by a factor of about 4 in 2 days (giving a doubling time of about 2 days for the average standard deviation). In a recent study (Lorenz 1969), the growth rate of initial error has been estimated by following the behavior of two closely resembling states of the atmosphere, and it is concluded that small errors would tend to double in about 2.5 days, in the root-mean-square sense. The present calculations appear to be in broad agreement with the conclusions of Lorenz obtained from a different approach.

VARIATION OF STATION DENSITY

The growth of initial uncertainty, as obtained here in terms of the increase in the variance of the analysis error, thus intimately depends upon the particular constant pressure level chosen, as the variance is directly proportional to the square of the gradient of the quantity that is being analyzed. The growth is also influenced by the choice of the model because of the various terms that are incorporated. Throughout this development, we have assumed that a, the square of the average distance between reporting stations, remains constant. As equation(1) suggests, the larger the value of a—which means the smaller the number of reporting stations—the larger will be the initial error in the interpolated value of a variable. Thus, increasing the number of reporting stations will tend to reduce initial errors and correspondingly reduce the variance of the forecast fields.

For obtaining an estimate of the reduction in variance, different values of a were chosen by hypothetically increasing the number of stations over the region of analysis. Assuming that the hypothetical increase in number of stations does not significantly change the synoptic analysis, mean standard deviations of initial and forecast fields of the three-level quasi-geostrophic model were calculated and plotted against the number of stations as shown in figure 10. Here, the upper half of the figure shows the variation of initial standard diviation with respect to different values of n, the number of stations, while the lower half of the figure shows similar variation for the final standard deviation at the end of 48 hr. The reduction in standard deviation is inversely proportional to the square root of the number of stations and yields about 30 percent reduction when the number of stations is doubled and about 43 percent when the number is trebled. Further increase in the number of stations produces a relatively smaller reduction in the standard

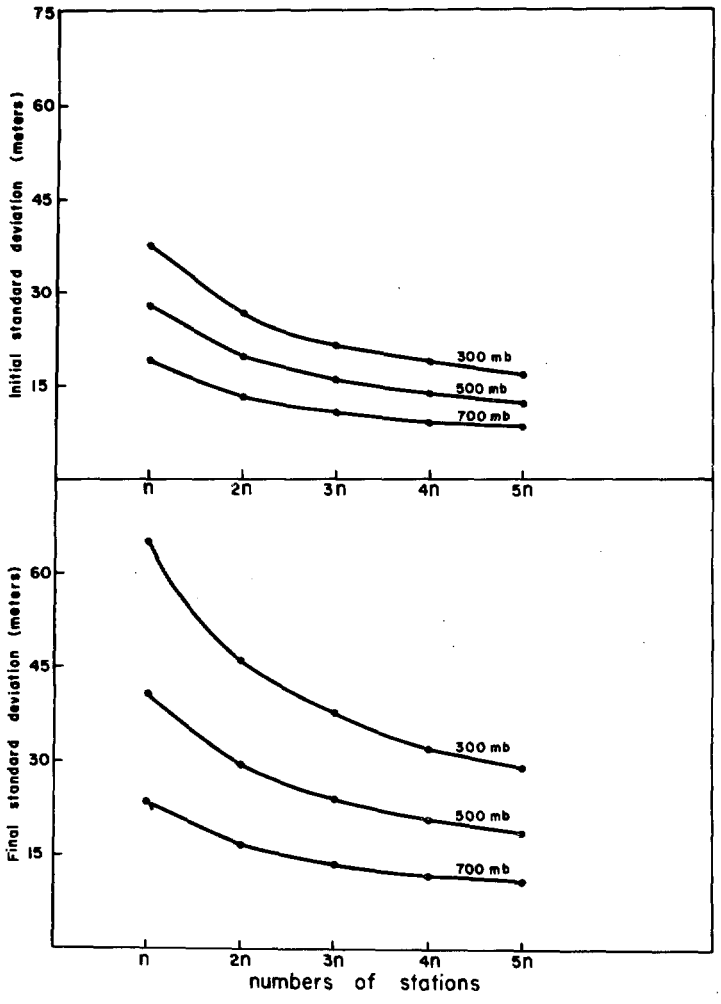

FIGURE 10.—Standard deviation of geopotential height error as a function of number of reporting stations; initial data, Jan. 25, 1964.

deviation. If we consider the cost of maintaining a station network as uniformly proportional to the number of stations, then we may conclude that the point of diminishing return is somewhere between $2n$ and $3n$, beyond which the reduction in error is too small to warrant increasing the station density. In reality, the increasing number of stations will reveal the smaller scale features of the atmosphere and will in general tend to increase the gradients of the analyzed field. The calculations made here on the assumption of no change in gradient lead us to the maximum possible reduction in error and thus give an upper limit to the possible gain that could be obtained by increasing the number of stations.

6. SUMMARY AND CONCLUDING REMARKS

A comparative study of analysis errors and their growth with time was made for some simple atmospheric models using similar boundary and initial conditions. A barotropic and two simple baroclinic models were used in this study, and data from three synoptic situations were utilized to make predictions up to a period of 48 hr on a rectangular grid covering a major portion of the Northern Hemisphere. By means of a network sampling theory, theoretical minimum variances in height fields of various isobaric levels were obtained. With the aid of governing equations of each model, these minimum variances were transformed to final variances of forecast fields. Gaussian distributions were used to transform these minimum variances to maximum probabilities of forecast fields to be within specified magnitudes of true fields.

Theoretical mean probabilities were higher everywhere than the observed ones, in support of the network sampling theory which purportedly provides limiting probabilities not to be exceeded. The difference between the curves of theoretical and observed probabilities was found to be larger at all levels for 48-hr forecast verification when compared with the corresponding 24-hr forecast verification. This result demonstrates the inadequacy of all models for forecasting over longer periods. Further, the growth of theoretical variances with time was found to depend on the choice of the isobaric level and the terms that were incorporated in the governing equations of the models. In general, the growth was observed to be more pronounced in more complex models that incorporated additional terms of the vorticity equation; for the two-level balance model, the doubling time of the average standard deviation was found to be about 2 days. The effect of increasing the station density indicated that a substantial reduction in initial and final variances is realized by increasing the number of reporting stations by two to three times the present number.

The development of the variance equation in this study is based on the assumption that a given synoptic situation is analyzed subjectively using the data obtained from reporting stations. In recent years, the usual conventional analysis is more and more replaced by an objective analysis that can be done on an electronic computer in much shorter time. One of the standard methods employed in an objective analysis obtains an estimate of a variable at any grid point in terms of a weighted linear combination of data from surrounding stations. In such a scheme, the initial uncertainty is in general a function of network density and the chosen set of weights. A selected set of weights defines a response function, and the initial uncertainty will in general be proportional to the fraction of the variance that remains unaccounted for by the response function. This procedure introduces systematic errors at every grid point that will grow with time and will in turn affect the forecast fields in a similar manner as do the errors from the conventional analysis. It is felt that a comparison of the distribution of initial uncertainties encountered in subjective and objective analyses may suggest a criterion for a proper choice of an objective analysis scheme.

The present study is limited to rather simple models of the atmosphere. In the last few years, meteorologists have considered more complex models, such as ones based on complete balance filter and primitive equations. It seems worthwhile to carry out a detailed error analysis of these models using various input levels. Such a study can be designed to assess the importance of various terms at different levels together with the initial uncertainties

associated with them. Further, we can determine the growth rates of initial uncertainties for individual terms of the governing equations by carrying out numerical integration in time. This may enable us to decide upon an optium physical model that would have the least growth of initial uncertainties for a given synoptic situation.

APPENDIX—DEVELOPMENT OF VARIANCE EQUATIONS IN VARIOUS MODELS

Consider first the simple barotropic model for which the vorticity equation is given by (3). When expressing this in finite-difference form for the central point 0 as shown in figure 11,

$$\dot{z}_1+\dot{z}_2+\dot{z}_3+\dot{z}_4-4\dot{z}_0=\tfrac{1}{4}[(z_2-z_4)(\eta_1-\eta_3)-(z_1-z_3)(\eta_2-\eta_4)]. \tag{11}$$

Further, expressing η, the absolute vorticity, at every grid point in terms of z and using the quasi-geostrophic assumption, we can expand this equation to write

$$\dot{z}_1+\dot{z}_2+\dot{z}_3+\dot{z}_4-4\dot{z}_0=\tfrac{1}{4}\left\{(z_3-z_1)\left[f_2-f_4+\frac{gm_0^2}{\bar{f}d^2}(z_6+z_7+z_8-z_{10}-z_{11}-z_{12})\right]+(z_2-z_4)\left[f_1-f_3+\frac{gm_0^2}{\bar{f}d^2}(z_5+z_6+z_{12}-z_8-z_9-z_{10})\right]\right\}. \tag{12}$$

In this equation, $\dot{z}$ is the height tendency, $\partial z/\partial t$, g the acceleration of gravity, d the grid distance, m the map scale factor, f the Coriolis parameter, and $\bar{f}$ is the average value of the Coriolis parameter taken over the region of analysis. A subscript indicates the grid point at which a variable is evaluated.

By procedures described elsewhere (Gleeson 1961), errors of tendencies on the left side of equation (11) can be represented in terms of initial-state errors of quantities on the right side. Squaring and averaging both sides of the error equation yields the variance equation

$$\begin{aligned}\sigma^2(\dot{z}_1)+\sigma^2(\dot{z}_2)+\sigma^2(\dot{z}_3)+\sigma^2(\dot{z}_4)+16\sigma^2(\dot{z}_0)&=\frac{0.056a}{16}\left\{\left[f_2-f_4+\frac{gm_0^2}{\bar{f}d^2}(z_6+z_7+z_8-z_{10}-z_{11}-z_{12})\right]^2\right.\\&\times[(z_1')^2+(z_3')^2]+\left[f_1-f_3+\frac{gm_0^2}{\bar{f}d^2}(z_5+z_6+z_{12}-z_8-z_9\right.\\&\left.-z_{10})\right]^2[(z_2')^2+(z_4')^2]+\frac{g^2m_0^4}{\bar{f}^2d^4}[(z_2-z_4)^2[(z_5')^2+(z_9')^2]\\&+(z_1-z_3)^2[(z_7')^2+(z_{11}')^2]+(z_2+z_3-z_1-z_4)^2[(z_6')^2+(z_{10}')^2]\\&\left.+(z_1+z_2-z_3-z_4)^2[(z_8')^2+(z_{12}')^2]\right\}.\end{aligned} \tag{13}$$

Here, $\sigma^2(\dot{z}_N)$ is the variance of $\dot{z}$ at a grid point N in figure 11, and z_N' represents the gradient of z at N; for example,

$$(z_1')^2=[(z_5-z_0)^2+(z_6-z_{12})^2]\frac{m_1^2}{4d^2}. \tag{14}$$

In developing the variance equation, the cross products of tendency errors at pairs of grid points are formed, but they were omitted from equation (13). It can be reasoned that, if these errors are correlated, the correlation will be positive, and this will in general increase $\sigma^2(\dot{z}_N)$. Thus, their neglect minimizes the tendency errors to some extent.

Initially, the right side of equation (13) can be computed using the initial values of z at different grid points. The equation can then be solved by a standard relaxation procedure to yield $\sigma^2(\dot{z})$ everywhere, leaving three grid points on all sides of the boundary. At every time step, the variance equation is solved in a similar way using the predicted values of z.

In the case of the three-level quasi-geostrophic model, equation (4) is used to obtain the variance equation. In this equation, there are additional terms that involve the variance of ω at different levels. To obtain the variance ω equation, we consider the quasi-geostropic ω equation (5) and express it in finite-difference form using the height values, z, at levels below and above the level where the ω equation is being solved. The procedure is quite straightforward and will not be repeated here. The solution of the variance ω equation is again obtained using a standard relaxation procedure.

The vorticity equation for the two-level balance model is written in terms of the stream function ψ. The variance of the stream function can be obtained from the initial variance of the z field making use of the balance equation. Having obtained the variance of the stream function, the variance of its tendency, that is, $\sigma^2(\partial\psi/\partial t)$, can be obtained in exactly the same way as the variance of the height tendency is obtained in the barotropic model.

VARIANCE OF THE FORECAST HEIGHT FIELD

As we integrate the vorticity equation using a constant time step T, we obtain the forecast heights at every time step, using forward time differences for the first time step and centered time differences for the subsequent time steps. Schematically, at any grid point, we can write the forecast equations as

$$z_1=z_0+T\left(\frac{\partial z}{\partial t}\right)_0 \quad \text{for the first time step,}$$

$$z_2=z_0+2T\left(\frac{\partial z}{\partial t}\right)_1 \quad \text{for the second time step,}$$

and

$$z_3=z_1+2T\left(\frac{\partial z}{\partial t}\right)_2 \quad \text{for the third time step,}$$

and so on. Here, the subscript indicates the time step, 0 indicating the initial time, 1 for the first time, and so on. The value of the constant time step T is used as 1 hr

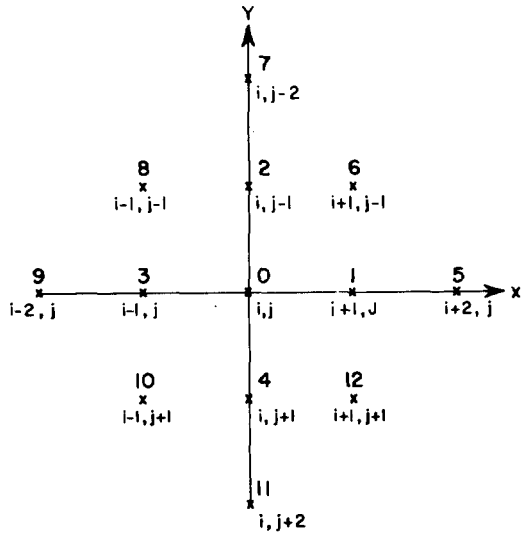

FIGURE 11.—Grid point arrangement for the finite-difference approximation of equations.

throughout. Combining these equations, we have

$$z_{2K}=z_0+2\,T\sum_{i=1}^{K}\left(\frac{\partial z}{\partial t}\right)_{2i-1} \quad \text{at the end of } 2K \text{ hr,}$$

and (15)

$$z_{2K+1}=z_0+T\left(\frac{\partial z}{\partial t}\right)_0+2\,T\sum_{i=1}^{K}\left(\frac{\partial z}{\partial t}\right)_{2i}$$

at the end of $2K+1$ hr.

Taking the variance of the above, we obtain

$$\sigma^2(z_{2K})=\sigma^2(z_0)+4\,T^2\sum_{i=1}^{K}\sigma^2\left(\frac{\partial z}{\partial t}\right)_{2i-1}$$

and (16)

$$\sigma^2(z_{2K+1})=\sigma^2(z_0)+\,T^2\,\sigma^2\left(\frac{\partial z}{\partial t}\right)_0+4\,T^2\sum_{i=1}^{K}\sigma^2\left(\frac{\partial z}{\partial t}\right)_{2i}.$$

In obtaining these equations, the cross-product terms are omitted as before, assuming that the errors in height tendencies at different time steps are uncorrelated. The neglect of the cross-product terms thus minimizes the variance.

Equations (16) enable us to obtain the variance of the forecast height field at any future time in terms of variance of the initial height field and variance of the height tendencies at different time steps.

The solution of all variance equations was obtained using a standard relaxation procedure and did not present any difficulties. At times, a few computed values of $\sigma^2(\dot{z})$ were found to be slightly negative. These values were found in the region of weak gradients where the magnitude of initial variance was very small. For simplicity, each negative $\sigma^2(\dot{z})$ was replaced by zero at that time step.

ACKNOWLEDGMENTS

I am deeply indebted to Dr. Thomas A. Gleeson for his constant encouragement and support throughout the course of this research work. Thanks are due Dr. D. W. Stuart for many helpful discussions. I wish to thank the Computing Center of the Florida State University for allotting free time to perform the computations of this research. Analyses of output fields obtained from various programs were done with the aid of a plotting routine of the Computing Center located at the National Center for Atmospheric Research in Boulder, Colo. I am grateful to Dr. John Gary of the NCAR Computing Center for making available the computer time and to Drs. James J. O'Brien and John Deluisi for their invaluable assistance during my stay in Boulder. Finally, appreciation is expressed to Mr. In ki Kim for his assistance in data collection.

REFERENCES

Cressman, George P., "Improved Terrain Effects in Barotropic Forecasts," *Monthly Weather Review*, Vol. 88, Nos. 9–12, Sept.–Dec. **1960**, pp. 327–342.

Gates, W. Lawrence, and Riegel, Christopher A., "Comparative Numerical Integration of Simple Atmospheric Models on a Spherical Grid," *Tellus*, Vol. 15, No. 4, Nov. **1963**, pp. 406–423.

Gleeson, Thomas A., "A Statistical Theory of Meteorological Measurements and Predictions," *Journal of Meteorology*, Vol. 18, No. 2, Apr. **1961**, pp. 192–198.

Gleeson, Thomas A., "Probabilities of Pressure Heights Forecast by Graphical and Numerical Methods," *Journal of Applied Meteorology*, Vol. 3, No. 5, Oct. **1964**, pp. 529–540.

Gleeson, Thomas A., "On Theoretical Limits of Predictability," *Journal of Applied Meteorology*, Vol. 6, No. 2, Apr. **1967**, pp. 213–215.

Leith, Cecil E., "Numerical Simulation of the Earth's Atmosphere," *Report*, Contract No. W-7405-eng-48, Lawrence Radiation Laboratory, University of California, Livermore, **1964**, 40 pp.

Lorenz, Edward N., "Energy and Numerical Weather Prediction," *Tellus*, Vol. 12, No. 4, Nov. **1960**, pp. 364–373.

Lorenz, Edward N., "The Predictability of Hydrodynamic Flow," *Transactions of the New York Academy of Sciences*, Ser. II, Vol. 25, No. 4, Feb. **1963**, pp. 409–432.

Lorenz, Edward N., "Atmospheric Predictability as Revealed by Naturally Occurring Analogues," *Journal of the Atmospheric Sciences*, Vol. 26, No. 4, July **1969**, pp. 636–646.

Mintz, Yale, "Very Long-Term Global Integration of Primitive Equations of Atmospheric Motions," *WMO Technical Note* No. 66, World Meteorological Organization, Geneva, **1965**, pp. 141–167.

Stewart, Dorathy A., "The Effect of Analysis Errors on Some Predictions Made With the Spectral Vorticity Equation," *Journal of Applied Meteorology*, Vol. 6, No. 4, Aug. **1967**, pp. 610–616.

Thompson, Philip D., "Uncertainty of Initial State as a Factor in the Predictability of Large Scale Atmospheric Flow Patterns," *Tellus*, Vol. 9, No. 3, Aug. **1957**, pp. 275–295.

[*Received October 13, 1969; revised April 3, 1970*]